

Investigation of the reproducibility of bladder dose- volume histogram (DVH) in prostate tomotherapy using the center of mass of the bladder in daily megavoltage computed tomography (MVCT) images

F. Goli-Ahmadabad¹, S.R. Mahdavi^{1,2*}, A. Nikoofar³, A. Zare-Sadeghi¹,
H. Vazirinasab^{4,5}, S. Bagherzadeh⁶, G. Esmaili⁷, N. Hasani⁷

¹Department of Medical Physics, School of Medicine, Iran University of Medical Sciences, Tehran, Iran

²Radiation Biology Research Center, Iran University of Medical Sciences, Tehran, Iran

³Department of Radiation Oncology, School of Medicine, Iran University of Medical Sciences, Tehran, Iran

⁴Department of Epidemiology and Biostatistics, School of Public Health, Kerman University of Medical Sciences, Kerman, Iran

⁵School of Public Health, Jiroft University of Medical Sciences, Jiroft, Iran

⁶Cellular and Molecular Biology Research Center, Larestan University of Medical Sciences, Larestan, Iran

⁷Department of Radiotherapy, Pars Hospital, Tehran, Iran

► Original article

*Corresponding author:

Seied Rabi Mahdavi, Ph.D.,

E-mail:

srmahdavi@hotmail.com

Received: November 2023

Final revised: January 2024

Accepted: February 2024

Int. J. Radiat. Res., January 2025;
23(1): 111-120

DOI: 10.61186/ijrr.23.1.111

Keywords: Prostate cancer, tomotherapy, DVH (dose volume histogram), bladder, reproducibility, mixed model.

ABSTRACT

Background: The DVH is the most used radiotherapy formulation. DVH plays a fundamental role in determining dose constraints and side effects. Volume also plays the main role in calculating DVH. In prostate treatment, there is no comprehensive consensus on determining the association between bladder volume (BV) and side effects. Our aim is to investigate the reproducibility of bladder DVH (DVHB). D50%BV (dose received by 50% of BV) is used to analysis DVHB. **Materials and Methods:** We contoured the bladder of 467 daily MVCT images of fifteen prostate cancer patients who underwent tomotherapy. Using R software 4.2.3, the correlation between the bladder center of mass (XCM, YCM, ZCM), BV with D50%BV were modeled by the mixed model. Two prediction models were presented for D50%BV, the first model was based on BV and (XCM, YCM, ZCM), the second model was based on BV. **Results:** Statistical analyses revealed that independent factors YCM, ZCM, and BV have a significant influence on the response variable D50%BV. According to mixed model, YCM has a positive correlation with D50%BV, while ZCM or BV has a negative correlation. XCM does not significantly affect D50%BV. Akaike Information Criterion (AIC) index indicated that first model has a higher goodness of fit than second one. **Conclusion:** Our findings demonstrate that bladder location also affects D50%BV, in addition to BV. It can be concluded that DVHB is not always repeatable as a scientific claim.

INTRODUCTION

Radiotherapy is one of the most important methods for the treatment of prostate cancer. The first goal of radiotherapy is to deliver the prescribed dose to the target, and the second goal is to reduce radiation to organs at risk (OAR), which can be accomplished by using image-guided radiotherapy (IGRT) and improving equipment accuracy^(1, 2). The IGRT framework is used to study OARs intra- and inter-fractionally⁽³⁾. The DVH is a significant and widely used definition for limiting radiation exposure to OARs. Clinically, the DVH is used to determine constraint doses. A correlation between DVH and clinical outcomes is required to explain acute and late effects. This correlation also explains dose constraints^(4, 5). The findings from the correlation of side

effects and DVH_B in prostate treatment vary greatly, and no comprehensive agreement has yet been reached^(3, 6-13). One of the most important characteristics of a scientific claim is the reproducibility of a scientific test^(14, 15). DVH_B must be reevaluated for these reasons. Is DVH_B reproducible if all treatment conditions for a patient are fixed, such as the prescribed dose, BV, treatment plan (TP), radiotherapy machine, and positioning during treatment? Is a patient's or a group of patients' DVH_B during treatment under completely fixed conditions solely dependent on BV? Our goal is to respond to these inquiries. According to the fact that prediction is an important criterion for scientific hypothesis⁽¹⁶⁾, we investigated DVH_B using two predictor models based on two approaches. To improve accuracy, we studied patients both individually and in groups. This

study investigates the reproducibility of bladder DVH_B in prostate tomotherapy and explores the correlation between bladder location and DVH_B. This aspect has not been thoroughly examined in prior scientific literature.

MATERIALS AND METHODS

Selection of patients

A retrospective analysis was conducted on all prostate cancer patients who underwent treatment at Pars Radiotherapy Center between 2019 and 2021, utilizing the Tomotherapy machine X9 (Accuray, USA). Patients with partial inclusion of the bladder in the MVCT images were excluded. Finally, eight patients received the prescribed dose of 69 Gy, three received 72 Gy, and four received 78.2 Gy. 15 patients treated using the simultaneous integrated boost (SIB) technique are:

Group1: patients 1 to 8 with a prescribed dose of 69 Gy

Group2: patients 9 to 11 with a prescribed dose of 72 Gy

Group3: patients 12 to 15 with a prescribed dose of 78.2 Gy

Preparation of patients

One hour before the CT-planning and MVCT procedures, patients were instructed by the physician to empty their bladders, consumed four 150 mL glasses of water at 15-minute intervals, and subsequently evacuate their bowels. The patients were irradiated while supine with knee support. Prior to each treatment session, an MVCT scan was conducted, and the MVCT image was aligned with the planning CT using the femur as a marker. The patient's bladder volume (BV) was checked out, and if the findings deviated from the initial plan, the patient was instructed to either void or fill their bladder once more. The MVCT imaging procedure was performed again within a time frame of 30 to 60 minutes.

Dose calculation on MVCT

To calculate the daily dose in the BV, the MVCT images were rigidly auto-aligned on the KVCT-plan image (or original plan) using MIM software version 6.1 (MIM Software Inc., Cleveland, OH, USA). For every patient in our study, we included one KVCT-plan image and a total of 28 to 36 MVCT images. Using MIM software, the bladders of 15 patients—a total of 467 MVCT and CT-planning images—were contoured. The software MIM was utilized to extract the data for BV, DVH_B, X_{CM}, Y_{CM}, Z_{CM}, and D_{50%Bv}. The coordinates (X_{CM}, Y_{CM}, Z_{CM}) represent the center of mass of the BV (figure 1). We chose D_{50%Bv} as a representative DVH_B for the analysis of DVH_{Bs}.

We utilized R software version 4.2.3 to examine the correlation between D_{50%Bv}, X_{CM}, Y_{CM}, Z_{CM}, BV, and the treatment group. We performed this task individually for each group, collectively for all groups, and cumulatively for the combined total of all three groups.

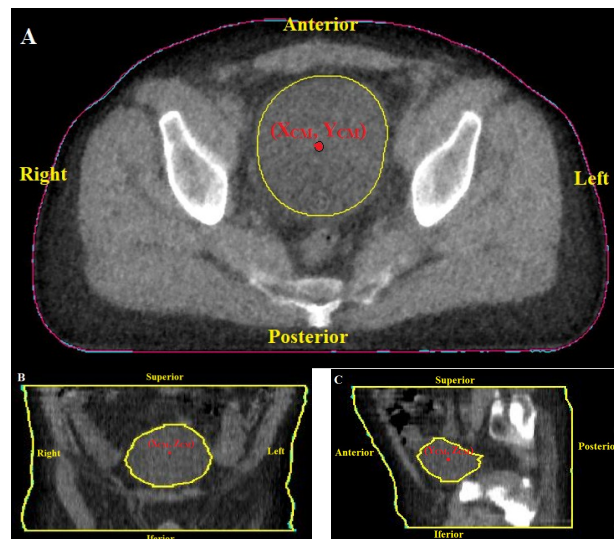


Figure 1. Center of mass contoured bladder of one patient using MVCT image: **A.** Axial, **B.** Coronal, **C.** Sagittal, is from left to right (laterally), is from anterior to posterior, and is from inferior to superior in MIM software.

Statistical analysis

In the first step, with the backward method, a linear equation was created between D_{50%Bv} (the response variable) and predictor variables (X, Y, Z, and volume) for each group and the whole data, and then the model was estimated (figure 2). In the second step, we used mixed regression to add random effects (individual-specific effects) to the final linear regression model in the previous step. The random effect of an independent variable means the existence of different coefficients for a variable for each person in a group, but the fixed effect of an independent variable means the existence of a coefficient for a variable for all people in a group. It can be said that fixed effects indicate the characteristics of a group and random effects indicate the characteristics of an individual. Intra-class correlation (ICC) was used to report random effects, and a larger Adjusted ICC indicates the performance of mixed regression versus linear regression. In the last step, we compared the final model resulting from the mixed regression (the first model) with the volume-based regression model (the second model) using the AIC index. A model with a better fit has a lower Akaike index. Prior to their inclusion in the regression analysis, we used a process of standardization to all variables. The analyses were performed utilizing R software version 4.2.3.

RESULTS

The investigation included a retrospective enrollment of 15 patients who had been diagnosed with prostate cancer. The number of imaging instances per patient varied from 29 to 37. The collective data obtained from the therapy sessions of the 15 patients in the study yielded a total of 467 data points. Among these, 247 data points were attributed to 8 patients in the first treatment group, 92 data

points were associated with 3 patients in the second treatment group, and 137 data points were linked to 4 patients in the third treatment group. Table 1 displays the largest and smallest bladder volumes of the patients, which can be compared to the bladder volume of the treatment plan. In order to visually represent the distribution of the dose in the bladder, one can also observe the maximum, minimum, and mean doses.

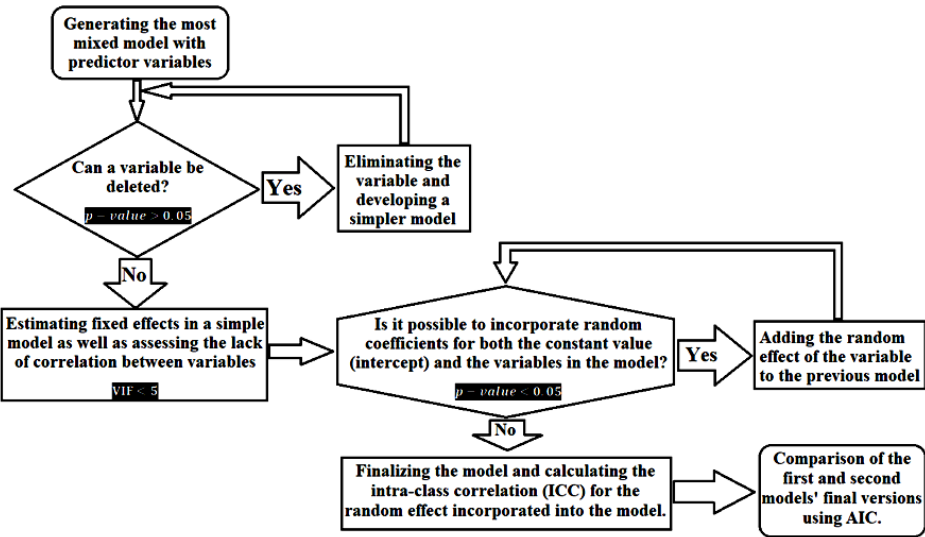


Figure 2. Flowchart of statistical analysis to generate a mixed model for predicting bladder D50%Bv based on two different concepts: the variables of the first model include XCM, YCM, ZCM and bladder volume (BV); The variables of the second model include only BV. VIF: variance inflation factor. AIC: Akaike Information Criterion.

Table 1. Charisticts of patients with prostate cancer who underwent treatment using tomotherapy.

Patient No.	Prescripti on Dose (Gy)	BV _{plan}				BV _{min}				BV _{max}				PSA (ng/ml)	Age	Prostatectomy
		Volume (mL)	D _{max} (Gy)	D _{min} (Gy)	D _{mean} (Gy)	Volume (mL)	D _{max} (Gy)	D _{min} (Gy)	D _{mean} (Gy)	Volume (mL)	D _{max} (Gy)	D _{min} (Gy)	D _{mean} (Gy)			
1	69	100.18	74.52	26.19	52.88	51.31	74.35	26.35	50.45	291.97	74.43	16.17	43.3	2.55	69	yes
2	69	121.04	72.25	15.45	50.35	83.38	72.1	15.73	51.68	124.54	72.24	15.6	49.57	1.55	82	no
3	69	132.19	70.77	33.38	51.81	76.42	70.73	33.97	52.86	689.25	70.69	29.56	44.26	7.42	59	no
4	69	105.3	73.16	24.67	51.25	70.3	72.99	24.82	50.42	211.64	72.85	21.33	46.5	4.22	69	yes
5	69	228.35	72.9	25.65	47.37	100.53	72.78	26.06	50.38	467.07	72.83	25.03	45.27	1.04	62	yes
6	69	154.4	73.75	10.01	39.69	91.01	73.6	10.96	45.22	364.18	73.43	10.04	35.73	0.21	55	yes
7	69	204.53	73.78	18.85	42.67	103.83	73.79	20.36	48.09	343.05	73.82	18.92	38.98	4.1	78	yes
8	69	159.88	72.14	14.68	36.01	101.61	72.12	15.28	40.98	279.44	72.08	14.69	35.75	0.28	58	yes
9	72	155.57	75.58	2.11	30.28	56.1	75.84	3.21	24.31	232.61	74.97	1.34	26.36	13	75	no
10	72	143.49	77.3	4.53	36.94	71.89	77.23	4.81	39.45	286.08	77.33	2.06	27.67	8	55	no
11	72	117.88	75.84	16.25	42.85	94.14	75.93	16.21	43.85	307.89	76.24	15.37	38.04	3	59	no
12	78.2	343.9	84.11	1.11	22.05	104.25	83.94	9.55	44.88	544.96	82.85	0.68	12.9	1	56	no
13	78.2	295.79	82.76	2.22	32.31	88.83	81.01	13.52	49	498.4	82.58	1	19.22	0.42	72	no
14	78.2	93.45	81.84	7.39	29.91	76.95	82.56	7.42	31.95	188.13	82.41	1.87	22	6	69	no
15	78.2	136.88	82.33	7.28	36.36	79.04	82.94	10.37	48.7	319.58	83.11	3.01	32.89	9.35	62	no
Mean	72.05	166.19	76.20	13.98	40.18	83.30	76.12	15.91	44.81	343.25	76.12	11.78	34.56	4.14	65.33	Yes ≈ 67%
SD	1.04	18.80	1.14	2.62	2.41	4.29	1.14	2.28	2.05	38.63	1.15	2.50	2.82	0.99	2.26	No ≈ 33%

BV_{plan}, Bladder Volume of the original plan; BV_{min}, Minimum bladder volume; BV_{max}, Maximum bladder volume, PSA, prostate-specific antigen

Assessment of DVH plots

In this study, all DVH_B patients were examined, and intentionally, some of them were drawn for better visibility (figure 3). Three important aspects were observed in the results: The same BVs from the same patient resulted in very different DVH_Bs, indicating a lack of reproducibility of the test; 2) As BV increases, DVH_B is expected to decrease, but

contrary to expectation, an increase in BV sometimes results in an increase in DVH_B, suggesting that a parameter other than BV plays a role in DVH_B; 3) Some DVH_B curves with different BVs of the same patient overlap, and it can be seen that there is no regular pattern when comparing two DVH_B curves of the same patient with increasing BV, D_x % (dose absorbed by X% of volume).

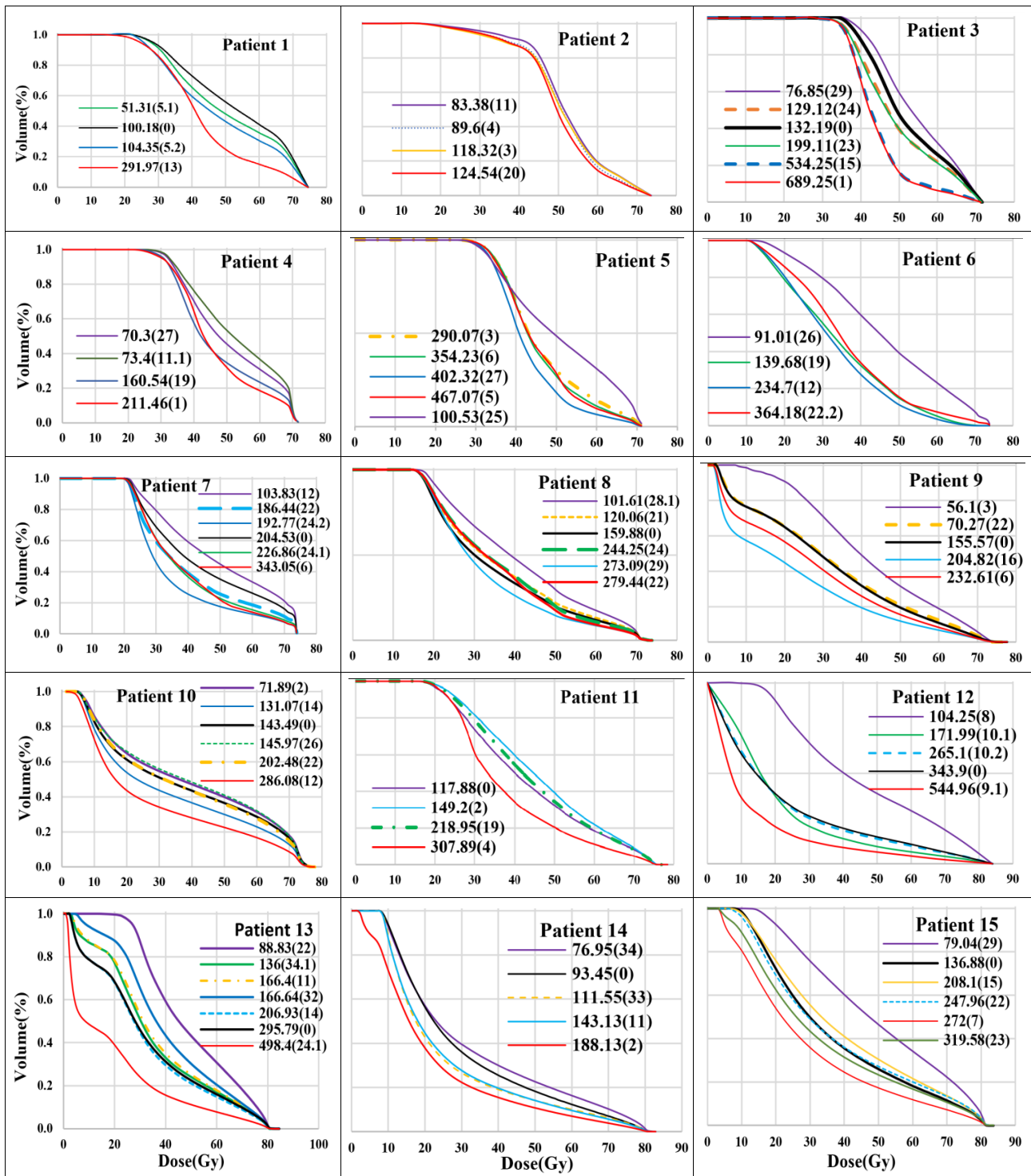


Figure 3. Dose volume histogram of bladder (DVHB) during prostate tomotherapy. 1 to 8 first group, 9 to 11 second group, 12 to 15 third group. The BV (ml) is sorted from smallest (purple) to largest (red), indicating in parentheses the treatment session number and the number after the first or second image control in the same treatment session. Session zero (black) shows the original plan.

Equations obtained from the first model

In this study, according to table 2, three equations were presented for groups 1, 2, and 3, and one equation for all three groups:

$$D_{(50\%BV)} \sim \begin{cases} \text{Intercept}_i + Y_{CM} + Z_{CM} + Z_{CMi} & (\text{Group 1}) \\ \text{Intercept}_i + Y_{CM} + Z_{CM} + \text{Volume} & (\text{Group 2}) \\ \text{Intercept}_i + Y_{CM} + Z_{CM} + \text{Volume} + Y_{CMi} & (\text{Group 3}) \\ \text{Intercept}_i + \text{Intercept} + Y_{CM} + Z_{CM} + \text{Volume} + \text{Volume}_i + \text{Group} & (\text{Total}) \end{cases}$$

The constant values of random effects (Intercept) and the coefficients of random effects (Z_{CMi} and Y_{CMi}) were calculated for each patient in groups 1, 2, and 3. The fixed effects coefficients (Y_{CM} , Z_{CM} and Volume) were calculated for each group and are shown in table 3. The predicted outcomes of these equations are displayed in figure 4.

Table 2. The process of obtaining the final mixed regression equation, as depicted in figure 2, involves following a series of steps. The random effect is represented by the index i.

	Factor in Model	AIC	Log Likelihood	Likelihood Ratio χ^2	Df of χ^2	p-value
Group 1	Volume, X_{CM} , Y_{CM} , Z_{CM}	141.63	-63.814	0.458	1	0.499
	X_{CM} , Y_{CM} , Z_{CM}	140.09	-64.043			
	Factor Volume removed of Model					
	X_{CM} , Y_{CM} , Z_{CM}	140.09	-64.043	2.185	1	0.139
	Y_{CM} , Z_{CM}	140.271	-65.135			
	Factor X_{CM} removed of Model					
	Y_{CM} , Z_{CM}	140.271	-65.135			
	Y_{CM} , Z_{CM} , Z_{CMI}	94.361	-40.181	49.908	2	<0.001
Group 2	Factor Z_{CMI} Added to Model					
	Final Model in Group 1: $D_{50\%BV} \sim \text{Intercept}_i + Y_{CM} + Z_{CM} + Z_{CMI}$					
	Volume, X_{CM} , Y_{CM} , Z_{CM}	114.67	-50.338	0.448	1	0.503
	Volume, Y_{CM} , Z_{CM}	113.12	-50.562			
Group 3	Factor X_{CM} removed of Model					
	Volume, Y_{CM} , Z_{CM}	105.98	-45.991	0.098	1	0.754
	Volume, Y_{CM} , Z_{CM}	104.08	-46.040			
	Factor X_{CM} removed of Model					
	Volume, Y_{CM} , Z_{CM}	104.08	-46.040			
	Volume, Y_{CM} , Z_{CM} , Y_{CMI}	98.72	-41.36	9.36	2	0.009 ^b
Total	Factor Y_{CMI} Added to Model					
	Final Model in Group 3: $D_{50\%BV} \sim \text{Intercept}_i + Y_{CM} + Z_{CM} + \text{Volume} + Y_{CMI}$					
	Volume, X_{CM} , Y_{CM} , Z_{CM} , Group Treatment	141.41	-61.703	0.633	1	0.426
	Volume, Y_{CM} , Z_{CM} , Group Treatment	140.04	-62.020			
	Factor X_{CM} removed of Model					
	Volume, Y_{CM} , Z_{CM} , Group Treatment	140.04	-62.020			
Total	Volume, Y_{CM} , Z_{CM} , Group Treatment, Volume _i	-68.702	44.351	212.74	2	2.2e-16 ^a
	Factor Volume _i Added to Model					
	Final Model in Total: $D_{50\%BV} \sim \text{Intercept}_i + \text{Intercept} + Y_{CM} + Z_{CM} + \text{Volume} + \text{Volume}_i + \text{Group}$					

Significance codes: 0 'a', 0.001 'b', 0.01 'c' and 0.05 'd', AIC: Akaike Information Criterion, Df of χ^2 : Degree of freedom χ^2

Table 3. Estimating regression coefficients for fixed and random effects in the mixed regression of the first and second models by treatment group and comparing them using Akaike's index. The random effect is represented by the index i.

		First Model		Second Model	
GROUP 1	Factors in Model	Intercept _i	ICC Subjects 0.842	Intercept _i	ICC Subjects 0.816
		Z_{CM}	Coefficient (95%CI) -1.14[-1.68, -0.59] ^{-b} (VIF=1.03)	Volume	Coefficient(95%CI) -0.49[-0.69, -0.30] ^{-c}
		Y_{CM}	Coefficient (95%CI) 0.24[0.18,0.31] ^{-a} (VIF=1.03)	Volume _i	ICC Volume (within Subjects) 0.070
		Z_{CMI}	ICC Z (within Subjects) 0.141		
	Adjusted ICC	0.983		0.886	
GROUP 2	Factors in Mode	Intercept _i	ICC Subjects 0.031	Intercept _i	ICC Subjects 0.768
		Z_{CM}	Coefficient (95%CI) -0.76[-0.91, -0.50] ^{-a} (VIF=1.095)	Volume	Coefficient (95%CI) -0.48[-0.76, -0.19] ^{-c}
		Y_{CM}	Coefficient (95%CI) 0.21[0.08,0.35] ^{-a} (VIF=1.12)	Volume _i	ICC Volume (within Subjects) 0.027
		Volume	Coefficient (95%CI) -0.38[-0.47, -0.29] ^{-c} (VIF=1/03)		
	Adjusted ICC	0.031		0.795	
GROUP 3	Factors in Mode	Intercept _i	ICC Subjects 0.973	Intercept _i	ICC Subjects 0.849
		Z_{CM}	Coefficient (95%CI) -2.10[-2.91, -1.25] ^{-a} (VIF=3.37)	Volume	Coefficient (95%CI) -0.93[-1.01, -0.84] ^{-a}
		Y_{CM}	Coefficient (95%CI) 0.63[0.12,1.13] ^{-c} (VIF=1.09)		
		Volume	Coefficient (95%CI) -0.45[-0.61, -0.30] ^{-a} (VIF=3.33)		
	Adjusted ICC	0.989		0.849	
TOTAL	Factors in Mode	Z_{CMI}	ICC Y (within Subjects) 0.016		
		Adjusted ICC	98.7		150.7
		Intercept _i	ICC Subjects 0.90	Intercept _i	ICC Subjects 0.90
		Intercept	Coefficient (95%CI) 0.86[0.14, 1.63] ^{-c}	Volume	Coefficient(95%CI) -0.43[-0.54, -0.32] ^{-a}
		Volume	Coefficient (95%CI) -0.25[-0.36, -0.13] ^{-a} (VIF=1.15)	Volume _i	ICC Volume (within Subjects) 0.040
		Z_{CM}	Coefficient (95%CI) -0.54[-0.76, -0.32] ^{-a} (VIF=1.21)		
		Y_{CM}	Coefficient (95%CI) 0.29[0.24, 0.34] ^{-a} (VIF=1.03)		
		Group2(ref: Group1)	Coefficient (95%CI) -1.40[-2.89, 0.04] ^{-c} (VIF=1.06)		
TOTAL	Factors in Mode	Group3 (ref: Group1)	Coefficient (95%CI) -2.14[-3.54, -0.84] ^{-a} (VIF=1.06)		
		Volume _i	ICC Volume (within Subjects) 0.048		
		Adjusted ICC	0.948		0.940
	AIC	-68.702		67.902	

Significance codes: 0 'a', 0.001 'b', 0.01 'c' and 0.05 'd', ICC: Intra Class Correlation, VIF: variance inflation factor

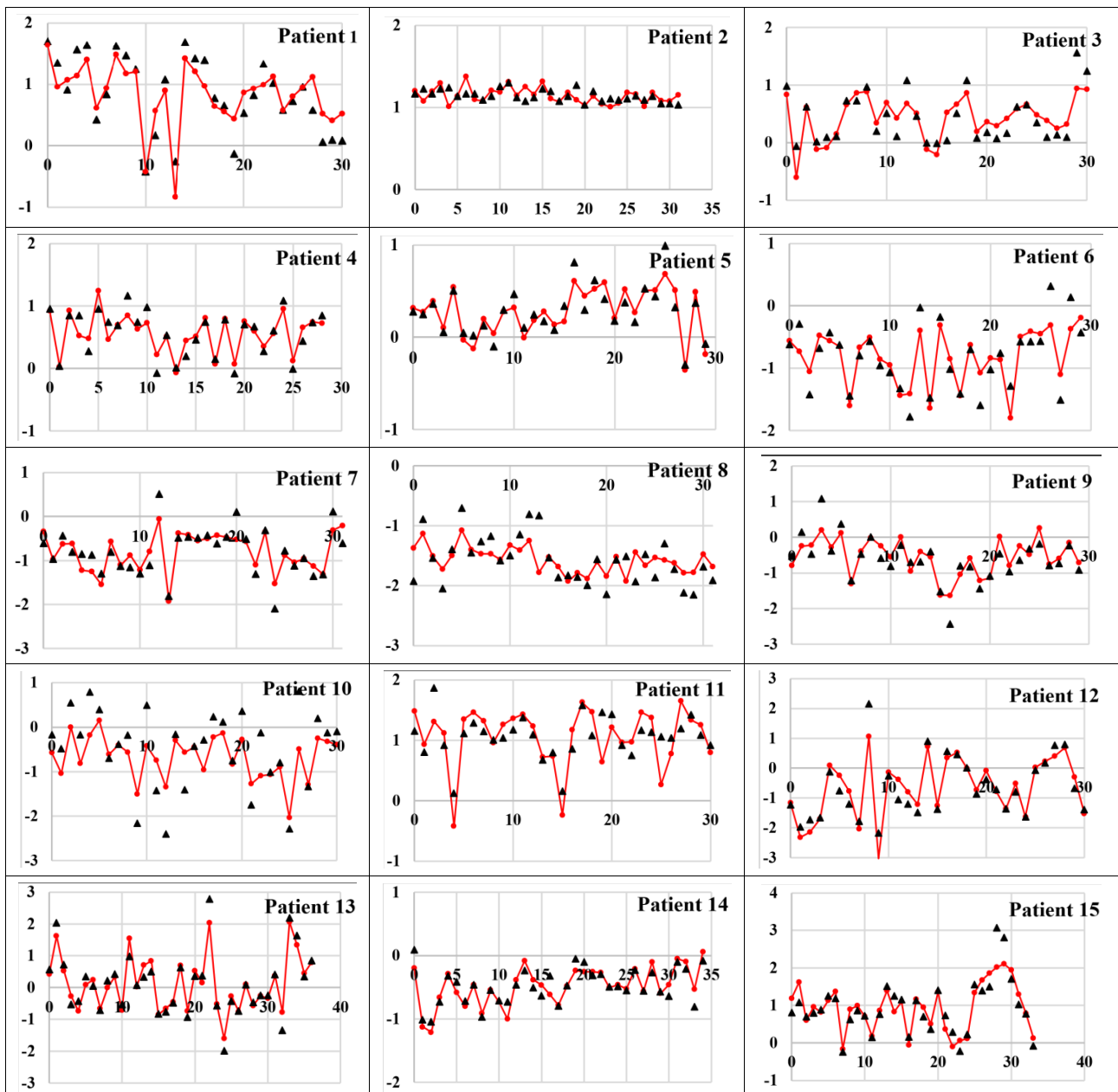


Figure 4. The vertical axis shows the standardized D50%BV and the horizontal axis shows the treatment session. The black triangles show D50% of the contoured bladder with the software MIM (or the actual observed values of D50%BV), the red circles show the values of the D50%BV of the prediction model with the first model.

Investigation of factors associated with $D_{50\%BV}$

The model incorporated X_{CM} , Y_{CM} , Z_{CM} , and BV as independent factors, while $D_{50\%BV}$ was designated as the response variable within each treatment group. The process leading to the derivation of the ultimate equation is documented in table 2. The table comprises a collection of noteworthy equations. As seen from the observations, the first group exhibits a correlation between $D_{50\%BV}$ and the fixed effects of Y_{CM} and Z_{CM} , along with a random effect of Z_{CMi} . The model in the second group, which incorporated fixed effects of volume, Y_{CM} , and Z_{CM} , exhibited the most optimal fit to the data. In the third group, along with the statistically significant fixed effects of variables Y_{CM} and Z_{CM} , as well as volume, it has been seen that the random effect of volume is also significant. At the

overall level of data analysis, the model incorporates X_{CM} , Y_{CM} , Z_{CM} , BV, and treatment group as independent variables. It was observed that all independent variables, except for X_{CM} , exhibited a statistically significant impact on the prediction of $D_{50\%BV}$. Additionally, it was shown that the random effect of volume exhibited statistical significance.

Correlation between predictor variables and $D_{50\%BV}$

To analyze the correlation between the independent variables within each group and the variable $D_{50\%BV}$, please consult table 2. The results indicate that within the first group, variables Z_{CM} and Y_{CM} exhibit contrasting weights in their ability to predict $D_{50\%BV}$. The level of $D_{50\%BV}$ grows as the value

of Y_{CM} increases and the value of Z_{CM} lowers. While the observed impact of variable Z_{CM} has a greater size, it is accompanied by a broader range of uncertainty, as indicated by its wider confidence interval. Additionally, the level of statistical significance associated with this effect is comparatively smaller. The mixed model accounted for 98.3% of the total variance within the group.

In the context of the second treatment group, when examining the model, it is observed that the mixed model exhibits characteristics akin to linear regression. Furthermore, the ICC value derived from the model indicates that merely 3% of the variance between clusters (individuals) can be accounted for. Hence, it can be concluded that there is no statistically significant random effect observed within this particular group. The correlation between volume and Z_{CM} in reference to $D_{50\%BV}$ is positive, whereas it is negative with respect to Y_{CM} . Furthermore, the impact of volume, in terms of both its magnitude and significance, is somewhat lesser when compared to the other two effects within this particular group.

Likewise, within the third treatment group, comparable to the second group, there exists a positive correlation between volume and Z_{CM} with respect to $D_{50\%BV}$; however, a negative correlation is observed between volume and Y_{CM} . The random effect of volume is also observed to be statistically significant within this group. By utilizing a mixed model, the model has successfully accounted for 98.3% of the total variance.

The findings of the mixed model analysis for predicting $D_{50\%BV}$ at the overall data level are presented below: There exists a notable negative correlation between the variables volume and Z_{CM} with the parameter $D_{50\%BV}$, but the variable Y_{CM} exhibits a noteworthy positive correlation with $D_{50\%BV}$. The coefficient values in table 3, together with their corresponding 95% confidence intervals, are presented. The coefficient associated with the impact of variable Z_{CM} exhibits a greater magnitude compared to the coefficients of the other variables.

Furthermore, it has been noted that in the second treatment group, as opposed to the first, the value of $D_{50\%BV}$ is lower by 1.40 units. This disparity is deemed statistically significant at a significance level of 1% ($P < 0.01$). In the third treatment group, the $D_{50\%BV}$ value is seen to be 2.14 units lower compared to the first treatment group. Furthermore, this disparity is shown to be statistically significant, with a p-value approximately equal to 0. The variance inflation factor (VIF) values for all the models show that the independent variables are not partially multicollinear.

Comparison between the first model and the second model

By utilizing the data presented in table 3, we may

further analyze and contrast the first model with the second one. Based on the AIC values, it is safe to say that the model that takes into account both the bladder's volume and location has consistently shown better optimality and a higher level of goodness of fit across all treatment groups. Figure 5 visually displays the AIC values for both models within each treatment group.

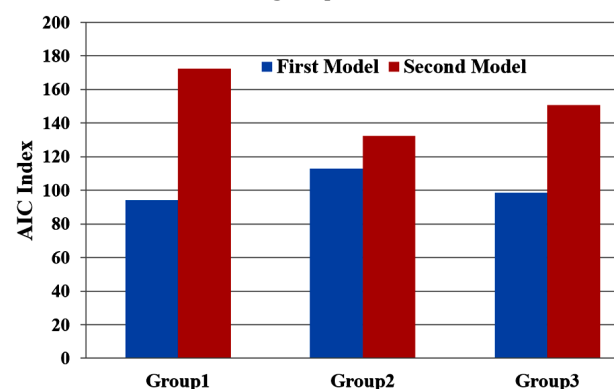


Figure 5. Comparison of the first and second models using the Akaike index.

DISCUSSION

Currently, there is no consensus on the volume-dose threshold for GU toxicity in prostate radiotherapy (11). Previous studies have shown that DVH_B parameters are not suitable for predicting bladder side effects (2, 17). According to Pinkawa et al.'s research findings (18), figure 3 unexpectedly shows that the increase in BV caused an escalation of the dose, likely causing the bladder to enter the high dose region. Unexpectedly, a significant decrease in BV resulted in a significant dose reduction (patient 1). The initial findings in figure 3 indicate that bladder volumes or drinking protocols are not effective predictors of DVH_Bs, which shows the unreliability of DVH_Bs. Additionally, it suggests that prescribed constraint doses for the bladder may not always be reliable, which aligns with previous research (2, 17, 19). However, in order to provide a scientific explanation for this problem, it is necessary to conduct thorough statistical analyses. It appears that no substantial documentation has been presented so far. In order to achieve this objective, we conducted an analysis on $D_{50\%BV}$, which serves as a representative of DVH_Bs.

We presented two models to predict $D_{50\%BV}$: the first model based on BV and (X_{CM} , Y_{CM} , Z_{CM}), and the second model based only on BV. The first model is grounded on an innovative hypothesis that incorporates considerations of the bladder's spatial positioning, which is the first time in this study. The objective of this study is to offer an explanation for the lack of reproducibility observed in DVH_Bs, as shown in figure 3. The statistical indicators show that the first model is better than the second model (table

3). In more concise terms, it can be inferred that the positioning of the bladder in the first model indicates that BV is not the sole determinant in the DVH formula.

The modeled equations (table 2) show that BV is not the only determining factor for $D_{50\%BV}$, so DVH_B is not always repeatable as a scientific claim. Finally, we have shown that $D_{50\%BV}$ or DVH_B also depends on the Y_{CM} and Z_{CM} of the bladder (or location of the bladder). The fixed and random effects in these equations represent the group and individual characteristics of patients.

The fixed effects relate to coefficients that exhibit uniformity across all individuals within a group or statistical population. In essence, these coefficients are applicable to all patients. The lack of variable X_{CM} in the equations suggests that the bladder could be undergoing symmetrical expansion or contraction in the lateral direction. The presence of Y_{CM} with a positive coefficient (table 3) in all four equations indicates that the motion of the bladder from the anterior to the posterior leads to an increase in $D_{50\%BV}$. The presence of Z_{CM} with a negative coefficient (table 3) indicates the motion of the bladder from the inferior to the superior leads to a decrease in $D_{50\%BV}$. The negative volume coefficient demonstrates the inverse correlation between $D_{50\%BV}$ and volume, indicating that as volume increases, $D_{50\%BV}$ decreases. The variable of group 2, when compared to group 1, resulted in a reduction of 1.4 units of $D_{50\%BV}$ in the total equation. Group 3, in comparison to group 1, exhibited a decrease of 2.14 $D_{50\%BV}$ (table 3). While the prescribed dose in the second and third groups for the prostate was increased, it led to a decrease in $D_{50\%BV}$, which can be attributed to the focus of the dose in the prostate region.

Random effects relate to individual characteristics that differ among patients. Put simply, these effects demonstrate that individual treatments can yield superior outcomes. The index i in the given equations denotes a specific effect related to an individual. The inclusion of an intercept _{i} factor in all equations with high ICC (table 3) in the first and second models indicates the existence of a consistent and distinct value for each patient. The variation in these constant values may be attributed to the distinct morphology and treatment planning of the patients. At present, the cause of these variations remains unknown, necessitating additional investigation.

The final models indicate that the $D_{50\%BV}$ is dependent on the bladder's location, as shown by the Y_{CM} and Z_{CM} . The final models can explain why the bladder may occasionally move in a different direction, according to Gurjar *et al.* (20). Despite BV changes and varying adherence to the bladder filling protocol, Smith *et al.* (21) show that a small bladder in the session image is not the reason why the mandatory dose constraint is not met during therapy

in prostatic patients using MR-Linac. Nakamura *et al.* (22) did not find any association between variations in BV and acute cystitis. They also observed that some volumes above 150 ml could not reach the dose constraint. These studies clearly show a weak association between BV and DVH_B , but without a clear explanation, which can be seen repeatedly in our results (figure 3). The final models (table 2) demonstrate that the $D_{50\%BV}$ is influenced by both the location and volume of the bladder.

Constraint doses are determined through the utilization of the DVH and the assessment of associated side effects. If the DVH is not reproducible, it can have an impact on the accuracy of the side effects analysis. Put simply, it is not possible to establish a robust correlation between volumes and side effects. Multiple studies have demonstrated a lack of correlation between DVH_B and side effects (10, 17, 23). The final models demonstrate that Z_{CM} and Y_{CM} significantly influence the determination of DVH_B . Several studies have demonstrated that varying bladder volumes do not impact the late and acute effects (6, 8, 13). In the final models, Z_{CMi} , Y_{CMi} , and $volume_i$ represent the individual effect, or random effect, of each BV in patients. These effects may vary from one patient to another. Kupelian *et al.* (24) demonstrated that there can be variations in bladder changes between different patients.

The absence of consensus regarding bladder toxicity (25) and volume-dose thresholds for genitourinary (GU) toxicity (11) may be attributed to inadequacies in the definition of DVH. Although it's possible that additional variables (23, 26, 27) play a role in side effects, there is a strong likelihood that DVH_B is not always reproducible.

We compared the BVs of one patient, whose anatomical circumstances, treatment approach, and positioning were consistent throughout the treatment. This made our investigation more accurate than other studies, despite the smaller sample size. These documents indicate that it is highly likely that DVH_B cannot be a reliable scientific claim because it is not always reproducible. On the other hand, the DVH_B curves have a definite pattern when the BV differences are very large (figure 3), which implies that when BV increases, DVH_B curves are drawn downward, and vice versa. But it should be noted that even with 100% increases and decreases in BV, we did not always observe this definite pattern.

According to the study of Grün *et al.* (10), the uncertainty of BV is very high, and our study suggests that DVH_B may similarly have substantial uncertainty. Maybe these uncertainties aren't complicated in conventional treatments, but they can be important in stereotactic body radiotherapy (SBRT) treatments (28).

The occurrence of Y_{CM} or Z_{CM} can be attributed to alterations in the morphology or positioning of the

bladder. Through the identification of these factors, it is potentially feasible to enhance the reproducibility of DVH_B. The potential enhancement of accuracy in drinking water protocols can be attributed to the reproducibility of DVH_B. The extent to which Y_{CM} and Z_{CM} accurately represent alterations in bladder position or morphology remains uncertain, potentially impacting the accuracy of the investigation. However, it can be argued with high confidence that bladder position, independent of BV, can play an important role in DVH_B estimation. Mylona *et al.* (29) have indicated that the assessment of the absorbed dose area in the bladder can yield more accurate insights into the potential side effects associated with the bladder. Our hypothesis posits that the incorporation of the location of the bladder into the DVH formula (4) can yield more accurate information.

Prediction is considered to be an essential criteria for evaluating scientific claims (16). It can be said that a model that has a better prediction is more acceptable from a scientific point of view. With this assumption, the equations of the first model can be applied to ultrasonic probes to estimate D_{50%Bv} (30,31). This study signifies a novel endeavor, thus rendering it impossible to make comparisons with prior studies, which constitutes the main limitation in our research.

In summary, we presented two models for the prediction of D_{50%Bv}. The first model incorporates both bladder volume (BV) and bladder location, while the second model solely relies on BV. We find that the first model outperforms the second model. This suggests that regardless of BV, the location of the bladder affects the value of D_{50%Bv} or DVH_B. Our research indicates that the DVH_B lacks reproducibility, which is an important feature of a scientific model.

Funding: The Research Deputy of the Iran University of Medical Sciences provided financial assistance for the current work (grant number: 1400-2-104-21944).

Ethical considerations: The research conducted in this study adhered to the principles outlined in the Declaration of Helsinki and was approved by the Ethics Committee of Iran University of Medical Sciences (Ethical code No. IR.IUMS.FMD.REC.1402.337). Accordingly, written informed consent was taken from all participants before any intervention. The study was registered in Research Registry IUMS (identifier: 21944). This study was extracted from PhD thesis of Foad Goli Ahmadabad at the department of medical Physics of Iran University of Medical Sciences (Thesis No. 29 in medical School). The authors have fully complied with ethical issues, such as plagiarism, data fabrication, and double publication.

Conflicts of interest: The authors declare that they have no competing interests.

Authors contribution statement: Conceptualization SRM, FGA; Methodology SRM, AN, AZS, HV; Software FGA, HV, AN, GE, NH; Funding acquisition HV, FGA, AN, GE, NH; Writing - Original Draft SRM, FGA; Formal analysis HV; Investigation SRM, FGA, HV, SB; Project administration SRM; Resources SB, GA, NH; Data Curation GE, NH, SB; Validation AN, AZS; Writing - Review & Editing All authors.

REFERENCES

1. Alonso-Arrizabalaga S, González LB, Ferrando JVR, Peidro JP, Torrecilla JL, Meseguer DP, *et al.* (2007) Prostate planning treatment volume margin calculation based on the ExacTrac X-Ray 6D image-guided system: margins for various clinical implementations. *Int J Radiat Oncol Biol Phys*, **69**(3): 936-43.
2. Dolezel M, Odrázka K, Vaculikova M, Vanasek J, Sefrova J, Paluska P, *et al.* (2010) Dose escalation in prostate radiotherapy up to 82 Gy using simultaneous integrated boost. *Strahlentherapie und Onkologie*, **186**(4): 197.
3. Adamson J and Wu Q (2008) Prostate intrafraction motion evaluation using kV fluoroscopy during treatment delivery: a feasibility and accuracy study. *Med Phys*, **35**(5): 1793-806.
4. Drzymala R, Mohan R, Brewster L, Chu J, Goitein M, Harms W, *et al.* (1991) Dose-volume histograms. *Int J Radiat Oncol Biol Phys*, **21**(1): 71-8.
5. Lebesque JV, Bruce AM, Kroes AG, Touw A, Shouman T, van Herk M (1995) Variation in volumes, dose-volume histograms, and estimated normal tissue complication probabilities of rectum and bladder during conformal radiotherapy of T3 prostate cancer. *Int J Radiat Oncol Biol Phys*, **33**(5): 1109-19.
6. Mullaney LM, O'Shea E, Dunne MT, Finn MA, Thirion PG, Cleary LA, *et al.* (2014) A randomized trial comparing bladder volume consistency during fractionated prostate radiation therapy. *Pract Radiat Oncol*, **4**(5): e203-e12.
7. Chen Z, Yang Z, Wang J, Hu W (2016) Dosimetric impact of different bladder and rectum filling during prostate cancer radiotherapy. *Radiation Oncology*, **11**: 1-8.
8. Tsang YM and Hoskin P (2017) The impact of bladder preparation protocols on post treatment toxicity in radiotherapy for localised prostate cancer patients. Technical Innovations & Patient Support in *Radiation Oncology*, **3**: 37-40.
9. Pang EPP, Knight K, Hussain A, Fan Q, Baird M, Tan SXF, *et al.* (2018) Reduction of intra-fraction prostate motion-determining optimal bladder volume and filling for prostate radiotherapy using daily 4D TPUS and CBCT. *Tech Innov Pat Sup Radiat Oncol*, **5**: 9-15.
10. Grün A, Kawgan-Kagan M, Kaul D, Badakhshi H, Stromberger C, Budach V, *et al.* (2019) Impact of bladder volume on acute genitourinary toxicity in intensity modulated radiotherapy for localized and locally advanced prostate cancer. *Strahlentherapie und Onkologie*, **195**(6): 517-25.
11. Olsson CE, Jackson A, Deasy JO, Thor M (2018) A systematic post-QUANTEC review of tolerance doses for late toxicity after prostate cancer radiation therapy. *Int J Radiat Oncol Biol Phys*, **102**(5): 1514-32.
12. Braide K, Kindblom J, Lindencrona U, Månsson M, Hugosson J (2019) The value of a bladder-filling protocol for patients with prostate cancer who receive post-operative radiation: results from a prospective clinical trial. *Acta Oncologica*, **58**(4): 463-8.
13. Chetiyawardana G, Hoskin PJ, Tsang YM (2020) The implementation of an empty bladder filling protocol for localised prostate volumetric modulated arc therapy (VMAT): early results of a single institution service evaluation. *The British Journal of Radiology*, **93** (1114): 20200548.
14. Munafò MR, Nosek BA, Bishop DV, Button KS, Chambers CD, Percie du Sert N, *et al.* (2017) A manifesto for reproducible science. *Nature Human Behaviour*, **1**(1): 1-9.
15. Harris JK, Combs TB, Johnson KJ, Carothers BJ, Luke DA, Wang X (2019) Three changes public health scientists can make to help build a culture of reproducible research. *Public Health Reports*, **134**(2): 109-11.
16. Meehl PE (1967) Theory-testing in psychology and physics: A methodological paradox. *Philosophy of Science*, **34**(2): 103-15.
17. Chen MJ, Weltman E, Hanriot RM, Luz FP, Cecilio PJ, Da Cruz JC, *et al.* (2007) Intensity modulated radiotherapy for localized prostate

- cancer: rigid compliance to dose-volume constraints as a warranty of acceptable toxicity? *Radiation Oncology*, **2**: 1-7.
18. Pinkawa M, Asadpour B, Gagel B, Piroth MD, Holy R, Eble MJ (2006) Prostate position variability and dose-volume histograms in radiotherapy for prostate cancer with full and empty bladder. *Int J Radiat Oncol Biol Phys*, **64**(3): 856-61.
 19. Jorgo K, Ágoston P, Major T, Takácsi-Nagy Z, Polgár C (2017) Transperineal gold marker implantation for image-guided external beam radiotherapy of prostate cancer. *Strahlentherapie und Onkologie*, **193**(6): 452.
 20. Gurjar OP, Arya R, Goyal H (2020) A study on prostate movement and dosimetric variation because of bladder and rectum volumes changes during the course of image-guided radiotherapy in prostate cancer. *Prostate International*, **8**(2): 91-7.
 21. Smith GA, Dunlop A, Barnes H, Herbert T, Lawes R, Mohajer J, et al. (2022) Bladder filling in patients undergoing prostate radiotherapy on a MR-linac: The dosimetric impact. *Tech Innov Pat Sup Radiat Oncol*, **21**: 41-5.
 22. Nakamura N, Shikama N, Takahashi O, Ito M, Hashimoto M, Uematsu M, et al. (2010) Variability in bladder volumes of full bladders in definitive radiotherapy for cases of localized prostate cancer. *Strahlentherapie und Onkologie*, **186**(11): 637.
 23. Pederson AW, Fricano J, Correa D, Pelizzari CA, Liauw SL (2012) Late toxicity after intensity-modulated radiation therapy for localized prostate cancer: an exploration of dose-volume histogram parameters to limit genitourinary and gastrointestinal toxicity. *Int J Radiat Oncol Biol Phys*, **82**(1): 235-41.
 24. Kupelian PA, Langen KM, Zeidan OA, Meeks SL, Willoughby TR, Wagner TH, et al. (2006) Daily variations in delivered doses in patients treated with radiotherapy for localized prostate cancer. *Int J Radiat Oncol Biol Phys*, **66**(3): 876-82.
 25. Rowe LS, Mandia JJ, Salerno KE, Shankavaram UT, Das S, Escorcia FE, et al. (2022) Bowel and bladder reproducibility in image guided radiation therapy for prostate cancer: results of a patterns of practice survey. *Advances in Radiation Oncology*, **7**(5): 100902.
 26. Carillo V, Cozzarini C, Chietera A, Perna L, Gianolini S, Maggio A, et al. (2012) Correlation between surrogates of bladder dosimetry and dose-volume histograms of the bladder wall defined on MRI in prostate cancer radiotherapy. *Radiotherapy and Oncology*, **105**(2): 180-3.
 27. Matzinger O, Duclos F, Van den Bergh A, Carrie C, Villà S, Kitsios P, et al. (2009) Acute toxicity of curative radiotherapy for intermediate- and high-risk localised prostate cancer in the EORTC trial 22991. *European Journal of Cancer*, **45**(16): 2825-34.
 28. Lovelock DM, Messineo AP, Cox BW, Kollmeier MA, Zelefsky MJ (2015) Continuous monitoring and intrafraction target position correction during treatment improves target coverage for patients undergoing SBRT prostate therapy. *Int J Radiat Oncol Biol Phys*, **91**(3): 588-94.
 29. Mylona E, Acosta O, Lizée T, Lafond C, Crehange G, Magné N, et al. (2019) Voxel-based analysis for identification of urethrovessical subregions predicting urinary toxicity after prostate cancer radiation therapy. *Int J Radiat Oncol Biol Phys*, **104**(2): 343-54.
 30. Barillot I, Horiot J, Maingon P, Bone-Lepinoy M, Vaillant D, Feutray S (1994) Maximum and mean bladder dose defined from ultrasonography. Comparison with the ICRU reference in gynaecological brachytherapy. *Radiotherapy and Oncology*, **30**(3): 231-8.
 31. Simforoosh N, Dadkhah F, Hosseini S, Asgari M, Nasseri A, Safarinejad M (1997) Accuracy of residual urine measurement in men: comparison between real-time ultrasonography and catheterization. *The Journal of Urology*, **158**(1): 59-61.